Eur Biophys J (2000) 29: 125–133

ARTICLE

Michael Rappolt · Georg Pabst · Gert Rapp
Manfred Kriechbaum · Heinz Amenitsch
Christian Krenn · Sigrid Bernstorff · Peter Laggner

New evidence for gel-liquid crystalline phase coexistence in the ripple phase of phosphatidylcholines

Received: 24 November 1999 / Revised version: 25 February 2000 / Accepted: 25 February 2000

Abstract Experimental evidence supporting the hypothesis of gel-liquid crystalline phase coexistence in the stable ripple phase of diacylphosphatidylcholines has been obtained from time-resolved X-ray small- (SAXS) and wide-angle diffraction (WAXS) in the millisecond to second time domain. The pretransition of 1,2-dipalmitoyl-*sn*-glycero-3-phosphocholine (DPPC) exhibits a thin lamellar liquid crystalline intermediate phase (designated L_{α^*}) if driven far away from equilibrium by an infrared temperature jump (T-jump) technique. The findings can be described by a two-step model. (1) Instantaneously with the T-jump, an anomalously thin lamellar liquid crystalline intermediate phase (d = 5.6–5.8 nm) forms, coexisting with the original gel-phase $L_{\beta'}$. Within the first seconds, the lamellar repeat distance of the intermediate increases to a value of about 6.7 nm. A closer examination of these kinetics reveals two relaxation components: a fast process, proceeding within tenths of a second, and a slow process, on the time scale of a few seconds. (2) Finally, both the liquid crystalline and the gel-phase relax into the stable ripple phase $P_{\beta'}$. The total process time of the transition is nearly independent of the addition of NaCl, but varies strongly with the chain length of the lecithin species.

M. Rappolt (✉)[1] · G. Pabst · M. Kriechbaum · H. Amenitsch
C. Krenn · P. Laggner
Institute of Biophysics and X-ray Structure Research,
Austrian Academy of Sciences, Steyrergasse 17,
8010 Graz, Austria

G. Rapp
European Molecular Biology Laboratory,
Hamburg Outstation, c/o DESY, Notkestrasse 85,
22603 Hamburg, Germany

S. Bernstorff
Synchrotron Trieste (ELETTRA), Strada Statale 14,
km 163.5, 34012 Basovizza (TS), Italy

Present address:
[1] IBR Austrian Academy of Sciences,
c/o Syncrotron Trieste (ELETTRA),
Strada Statale 14, km 163.5, 34012 Basovizza (TS), Italy
e-mail: michael.rappolt@elettra.trieste.it

Key words Phosphatidylcholine · Temperature jump · Small-angle X-ray scattering · Wide-angle X-ray scattering · Sodium chloride

Abbreviations *DPPC* 1,2-dipalmitoyl-*sn*-glycero-3-phosphocholine · *DMPC* 1,2-dimyristoyl-*sn*-glycero-3-phosphocholine · *SAXS*, *WAXS* small- and wide-angle X-ray scattering · *T-jump* temperature jump

Introduction

Despite numerous efforts since its discovery more than two decades ago (Tardieu et al. 1973), the stable-ripple phase ($P_{\beta'}$) of saturated diacylphosphatidylcholines is still not fully understood, both regarding its structural nature and its way of formation. Under near-equilibrium conditions this transition typically occurs several degrees below the main transition temperature (Jørgensen 1995), in which the chain packing changes from a rectangular – quasi-hexagonal – to a hexagonal packing (Ruocco and Shipley 1982). The lipid chains remain mainly in the all-*trans* conformation, but spectroscopic techniques indicate that the transition is accompanied by an onset of rapid chain and head-group rotation about the long molecular axis, while below the pretransition only oscillatory motions exist (Marsh 1980; Shepherd and Büldt 1979). In parallel, the lamellar long-range organization of the gel-phase $L_{\beta'}$ (Wiener et al. 1989) transforms continuously into the modulated, rippled lamellar superstructure of the $P_{\beta'}$ phase (Rappolt and Rapp 1996; Sun et al. 1996; Wack and Webb 1989).

One question addressed in the present studies concerns the structural pathway of this transition between two non-affine geometries (Laggner 1993), in which the lattice symmetry changes from a one-dimensional to a two-dimensional monoclinic type. In small-angle X-ray experiments (SAXS) under near-equilibrium condition, where a series of identical samples were held at constant temperatures for two weeks (Laggner et al. 1991), a loss

of long-range order in the pretransition regime at 34.5 °C was seen. It has been concluded that this disorder results from a statistical distribution of interbilayer distances in this temperatures region. However, under slow scanning conditions, with a constant scan rate of 0.1 °C/min, no such loss of order or intermediate phase could be detected (Tenchov et al. 1989). Despite such low scan rates, it cannot be excluded that the structural relaxation times are still longer than the five to ten minutes allowed to pass through the transition temperature region. We argue that near the transition midpoint, owing to critical slowing down (Komura and Furukawa 1988), even this low scan rate leads to non-equilibrium effects, which might have caused the differences in the results. However, with a heating rate of 15 °C/min, the phosphatidylcholine/water aggregate is clearly not able to follow the usual near-equilibrium pathway (Rapp et al. 1993). The lipid chains remain in the quasi hexagonal packing of the $L_{\beta'}$ phase, also above the pretransition temperature, and the monoclinic lattice of the $P_{\beta'}$ phase does not find time to develop completely.

In this work, we have used the appropriate extreme, the jump-relaxation approach, by which the system is rapidly disequilibrated. The temperature jump (T-jump) is triggered by a millisecond infrared laser pulse, which instantly "shoots" the system through the thermal phase boundary. We found previously that the system responds to the high thermodynamic driving force by formation of a thin layer lamellar intermediate instantaneously after the T-jump, which provides an efficient pathway for relaxation into the rippled phase $P_{\beta'}$ (Laggner et al. 1991).

The major examination therefore aims at the changes in hydrocarbon chain conformation, which might transiently change in parallel with the superstructural arrangement, especially in the transient thin lamellar phase. We find that the wide-angle X-ray scattering (WAXS) patterns display a broad diffuse peak at about $1/0.460\ nm^{-1}$, indicating molten chains for the intermediate phase, although the final temperature was always below that of the main chain melting transition. In correspondence to the formation of a similar anomalously thin lamellar liquid-crystalline phase, which was found by the same means in the L_α phase region (Laggner et al. 1999), this intermediate phase is designated L_{α^*}. Another example, where the system responds with an affine intermediate state, i.e., again a thin L_α phase forms, is the non-affine lamellar-to-inverted-hexagonal transition in phosphatidylethanolamines (Laggner et al. 1991). Also there, the thin lattice forms very rapidly after the laser pulse (5 ms), whereas the nascent phase H_{II} with the lower symmetry forms only slowly after a lag period of about 20 ms on account of the thin intermediate lamellar liquid crystalline phase (>5 s). In contrast, T-jump experiments carried out on the main transition of phosphatidylcholines do not display any intermediate structure (Rapp et al. 1993). The final L_α phase formed almost immediately after the laser heating (10 ms). We note that in none of the systems studies did the T-jump technique introduce additional lattice disorder and thus, taking into account also the large area to interior volume ratio of the multilamellar vesicle systems, the build up of thermoelastic stress is unlikely.

Since in this study the L_{α^*} phase clearly does not originate from the familiar liquid crystalline phase L_α, its transient appearance supports a recently published model for the pretransition of Heimburg (2000), in which a coupling of the ripple formation with the chain melting transition is stated. In this sense, also the discovery of the sub-main transition (Jørgensen 1995; Pressl et al. 1997), which occurs in the ripple phase regime just a few tenths of a degree below the main transition, may imply that the $P_{\beta'}$ phase is not one but two structurally related, thermodynamically distinct phases. It is demonstrated that this subtle mesomorphism arises from a stepwise increase in the domains with molten hydrocarbon chains on the account of ordered chain domains.

Materials and methods

Sample preparation

DPPC (1,2-dipalmitoyl-*sn*-glycero-3-phosphocholine) purchased from Sigma (Deisenhofen, 99% purity) and from Avanti Polar Lipids (Alabaster, AL, >99% purity) was used without further purification. Multilamellar lipsomes were prepared by dispersing weighted amounts of lipids (20% w/w) in 0, 0.1, 0.5 a 1 M NaCl solution, respectively (Fluka, Neu Ulm; double quartz distilled water, with a specific resistance 18 MΩ cm) and incubating the dispersions at 56 °C for 1.5 h. Then the samples were repeatedly vortexed and incubated at this temperature. The sample were stored about one day in the fridge at 4 °C and thereafter incubated for several hours at room temperature to stabilize the $L_{\beta'}$ phase. In slow-scan diffraction experiments (0.1 °C/min) the samples displayed narrow, cooperative main transitions (Rappolt 1995) with typical transition widths ΔT_m (FWHM = 0.12–0.19 °C) which provided a guarantee that the lipid purity corresponds to the specification of >99% (Albon and Sturtevant 1978). Throughout all T-jump experiments performed here, no appreciable difference could be seen in the induced phase transitions between the Sigma and the Avanti samples.

Instrumentation and X-ray diffraction

For time-resolved X-ray diffraction experiments with DPPC dispersion in 0.1 M NaCl, a sample holder of stainless steal sealed with 25 μm thick mica windows was used, as described previously (Rappolt 1995). Fresh lipid dispersions were injected in the cell chamber with a remote-controlled syringe driver for each T-jump generated with an erbium-glass IR laser. The wavelength of

the laser is 1.54 μm, at which the absorption coefficient of water is 1.5 cm^{-1} (for details see Rapp and Goody 1991). The cell was mounted on a Peltier element to equilibrate the sample at the starting temperature before each T-jump. Each time-resolved experiment (one cycle) consisted of a series of 64 time frames of pattern detection, with the laser (pulse length 2 ms) triggered at the beginning of the fifth frame. The laser-pulse energy was 1.25 ± 0.04 J, resulting in an averaged T-jump amplitude ΔT of 6.4 ± 0.8 °C. The variation given for the T-jump amplitude derives mainly from the difficulty to precisely measure the energy deposited on the sample; however, the reproducibility of the T-jump amplitudes lies within 2%. To reduce the thermal gradient in the sample an aluminum-coated kapton foil was used to back-reflect the transmitted IR beam upon the first passage through the sample. The initial temperatures of the present experiments were 29.9, 33.2 and 34.1 °C, which were measured by a thermocouple in contact with the sample. The first four exposures of 1 s were used to record the equilibrium state of the sample at the initial temperature with high precision: these were followed directly after the laser pulse by six time frames at the maximal time resolution (20 ms) and the rest of the exposures being 100 ms long. Each experiment was repeated 10 times, i.e., every diffraction pattern was averaged over 10 cycles. Further, "single-shot T-jump experiments" (no cycling) were done on DPPC dispersions in 0, 0.5 and 1 M NaCl which were filled and sealed in 1-mm thick quartz capillaries held in a steel cuvette, which provides good thermal contact to the Peltier heating unit (Anton Paar, Graz). With a higher laser-pulse energy of 2.34 ± 0.07 J, T-jump amplitudes ΔT of 12 ± 1.5 °C were reached. The initial temperature was fixed in all these experiments to 27.5 °C, and the maximum time resolution for the first set of frames directly after the laser pulse was 4 ms.

Diffraction patterns were recorded on the synchrotron beamline X13 of the EMBL outstation at DESY in Hamburg (Hendrix et al. 1979), and on the Austrian SAXS beamline at ELETTRA in Trieste (Amenitsch et al. 1998; Bernstroff et al. 1998). X-ray small- and wide-angle powder diffraction patterns were recorded simultaneously using a data acquisition system as described in Rapp et al. (1995). In both stations, two one-dimensional position sensitive detectors (Gabriel 1977) were used to monitor the corresponding *s*-ranges of interest from about 1/50 nm^{-1} to 1/2 nm^{-1} and from 1/3 nm^{-1} to 1/0.6 nm^{-1}, respectively. The angular calibration of the detectors was determined by using the SAXS diffraction patterns of dry rat tail tendon collagen (*d*-spacing = 65 nm) and the WAXS diffraction patterns of *p*-bromobenzoic acid as references (Ohkura et al. 1972). Since the samples were in total only exposed for about 10 s, no radiation damage was expected. This was confirmed by random thin layer chromatography tests on silica gel plates (Merck, Darmstadt). The solvent used was chloroform/methanol/water (65/25/4).

Data analysis

The raw data of the time-resolved experiments were normalized for the integration time of each time frame, and the background was subtracted by means of polynomials. The diffraction patterns were analyzed both in the SAXS and WAXS regime independently by fitting the first-order Bragg reflections using a least squares method based on the Levenberg-Marquardt algorithm (Press et al. 1986). Of special interest in the small-angle regime was the coexistence region of the $L_{\beta'}$ and L_{α^*} phases, where the model function was given by the sum of two Lorentzians.

The time course of the different lipid phase fractions during the T-jumps was calculated from the respective areas of the corresponding WAXS reflections (Klug and Alexander 1974). The gel-phase reflections were fitted by a Lorentzian fixed at 1/0.424 nm^{-1} and the diffuse liquid crystalline peaks by a Gaussian fixed at 1/0.460 nm^{-1}. We note that this model is not appropriate to characterize the WAXS pattern in detail (Ruocco and Shipley 1982; Sun et al. 1994; Wiener et al. 1989), i.e., the intensity profiles of the $L_{\beta'}$ phase are only described to a first approximation, since the shoulder at about 1/0.418 nm^{-1} is not taken into account. However, for the given quality of the diffraction patterns, especially for those with exposure times in the millisecond range, this method is capable of determining the relative amount of gel-phase lipids to within 10%. For normalization, the fraction in the pure gel-phase $L_{\beta'}$ was taken as unity.

The time dependency of the *d*-spacings $d(t)$ during the relaxation process of the L_{α^*} phase has been modeled by a two-component exponential decay:

$$d(t) = d_0 - d_A \exp\left(-\frac{t}{\tau_A}\right) - d_B \exp\left(-\frac{t}{\tau_B}\right) \quad (d(t) \le d_0\, t \in (0, \infty]) \tag{1}$$

In this context, d_0 gives the *d*-spacing in the equilibrium phase, i.e., that of the $L_{\beta'}$ phase d_A and d_B are the amplitudes of each component and the corresponding time constants are denoted as τ_A and τ_B, respectively. One should note that for $t = 0$, which is set as the starting point of the relaxation, the above equations yields minimum *d*-spacing value of the L_{α^*} intermediate and that this model is valid only for this times where the actual *d*-spacing is smaller than or equal to d_0. Further, models with one and three components have been under test using variance analysis and the *F*-test, but have been found to fail in favor of the above proposed model.

Results

Wide-angle diffraction

Figure 1 gives an overview of the temporal evolution of the diffraction patterns in the WAXS regime in a rep-

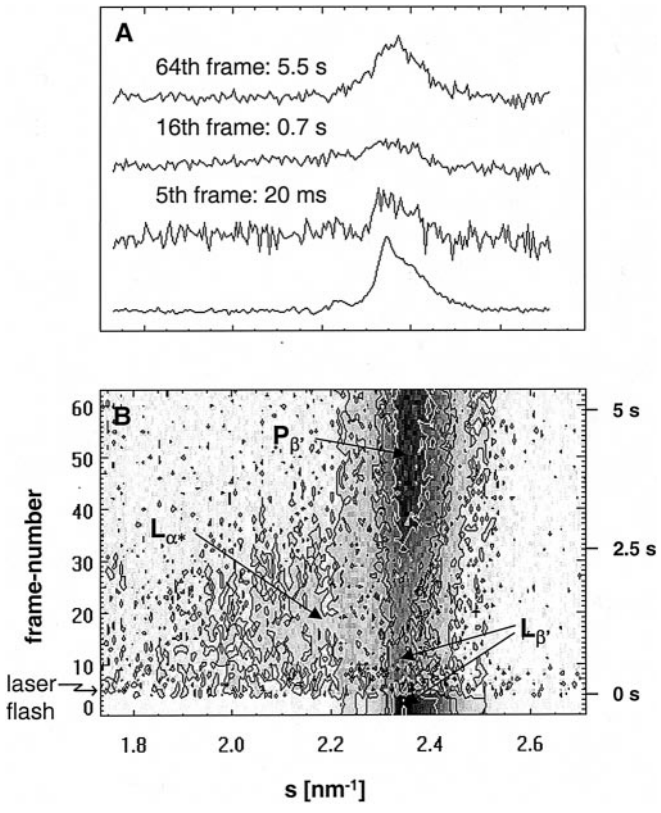

Fig. 1A, B Pretransition of DPPC (20% w/w in 100 mM NaCl) induced by a laser T-jump of 6.4 °C (T_i = 33.2 °C). **A** Four characteristic single diffraction patterns of the WAXS regime are extracted: before the T-jump (quasi-hexagonal packing of the chains), 20 ms and 0.7 s after the laser pulse (40 and 60% molten chains, respectively) and after 5.5 s (hexagonal packing of the lipid chains). **B** The temporal evolution of the diffraction pattern in the WAXS regime from $L_{\beta'} \rightarrow (L_{\beta'} + L_{\alpha^*}) \rightarrow P_{\beta'}$ is shown in the contour plot

resentative T-jump experiment with a start temperature of 33.2 °C. The first four frames that have been recorded before the T-jump correspond to the bottom pattern in the stack plot (Fig. 1A), showing the characteristic pattern of the quasi-hexagonal chain-packing of the $L_{\beta'}$ phase with a Bragg peak at 1/0.424 nm^{-1} and a shoulder at 1/0.418 nm^{-1}. Instantaneously, together with the T-jump in the 5th frame, the formation of molten chains is included, which is clearly seen by the increase of diffuse scattering around 1/4.6 nm^{-1} (see as indicated by the "L_{α^*} arrow" in Fig. 1B). However, not all the sample converts, but part of the gel phase remains in a quasi-hexagonal chain-packing after the T-jump (Fig. 1A, 2nd and 3rd patterns). In this experiment the main turnover to the ripple phase starts after approximately 0.9 s, wherein the lipid chains stiffen again. The equilibrium is reached after 3.3 s (Table 1). The Bragg reflection at 1/0.425 nm^{-1} indicates the hexagonal chain packing of the $P_{\beta'}$ phase (Fig. 1A, top pattern).

Figure 2 shows in three examples, differing in starting temperature T_i, the time course of the lipid phase fractions θ_β with all-*trans* conformation ($L_{\beta'}$ and $P_{\beta'}$ phases). After the laser pulse (vertical dashed line) the amount of the gel phase breaks down rapidly and continues to reduce until a

Table 1 Summary of the main parameters characterizing the pretransition of DPPC (100 mM NaCl) induced by a T-jump of 6.4 °C[a]

T_i(°C)	T_f(°C)	$T_f - T_p$(°C)	Δt_I (s)	Δt_{II} (s)	$\theta_{\alpha(max)}$
29.9	36.3	1.2	0.1	1.5	0.40
33.2	39.6	4.5	0.9	2.4	0.60
34.1	40.5	5.4	1.5	3.1	0.90

[a] The pretransition under non-equilibrium condition can be described in two steps: after the laser shot, in a first time interval Δt_I the maximum fraction of the intermediate phase L_{α^*} is reached and a second interval Δt_{II} from this point to the transition to the rippled phase takes place (compare to Fig. 2)

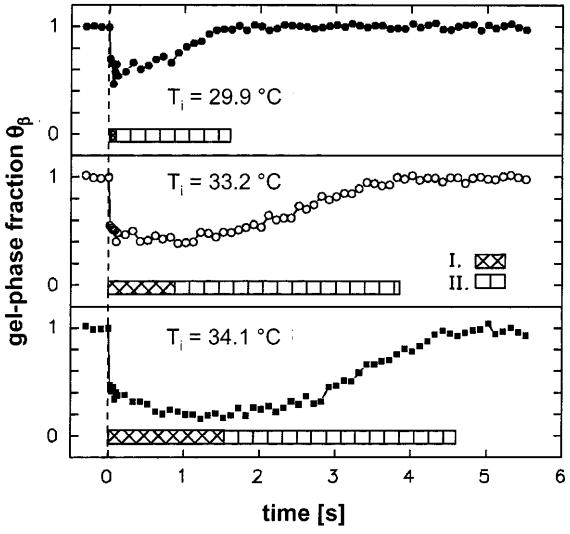

Fig. 2 Gel-phase fraction deduced from the WAXS regime during the pretransition of DPPC induced by an infrared laser. The first time interval Δt_I is defined from the laser shot until the maximum fraction of the intermediate-phase L_{α^*} is reached, and the second interval Δt_{II} from this point to the completion of the gel phase (for details see text and Table 1)

minimum quantity is reached (step I). As the starting temperatures T_i approach the pretransition temperature T_p = 35.1 °C (Rappolt 1995; Table 1) the time interval Δt_I for this step increases, whereas the minimum of θ_β decreases (Table 1). Concomitantly, the liquid-crystalline intermediate fraction increases, as higher final temperatures T_f are reached due to the constant T-jump amplitudes. In a second process (step II) the molten lipid chains return continuously to the all-*trans* conformation, as seen by the recovery of the gel-phase fraction θ_β (Fig. 2). The duration for this step increases with the surplus temperature $T_f - T_p$. We note, however, that the evaluated time intervals Δt_I and especially Δt_{II} from Table 1 have to be taken with care, since the passive cooling of the sample does affect the relaxation kinetics, e.g., in the used holder the sample cools down about 1 °C in 5 s.

Small-angle diffraction

Figure 3 displays the events in the SAXS regime for the same experiment as in Fig. 1. The initial $L_{\beta'}$ phase at

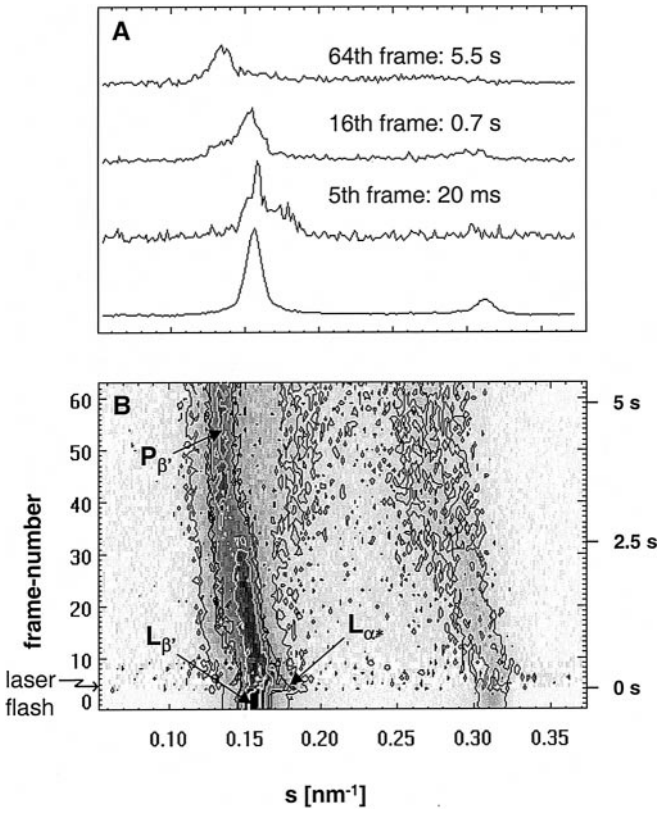

Fig. 3A, B This figure conforms to the same experiment as described in Fig. 1, presenting the SAXS data with exactly the same scheme. **A** Four characteristic single diffraction patterns of the SAXS regime are extracted. **B** The temporal evolution of the diffraction pattern in the SAXS regime from $L_{\beta'} \rightarrow (L_{\beta'} + L_{\alpha^*}) \rightarrow P_{\beta'}$ is shown in the contour plot

33.2 °C is represented by the first- and second-order Bragg peaks, for a *d*-spacing of 6.4 nm (Fig. 3A, bottom). The formation of the anomalously thin lattice of the L_{α^*} phase with a *d*-spacing 5.6–5.8 nm directly after the laser shot (5th frame) is seen in the contour plot of the first-order reflection, which displays a clear kink forward to higher angles (indicated by an arrow in Fig. 3B). The corresponding individual time-frame pattern in Fig. 3A demonstrates the coexistence of the $L_{\beta'}$ with the L_{α^*} phase, in agreement to the WAXS data. The major part of the sample remains in the $L_{\beta'}$ phase, as seen by the sharp Bragg peak at 1/6.4 nm^{-1}, and about 30–40% transforms into the L_{α^*} phase, as revealed by a relatively broad but well-defined peak around 1/5.7 nm^{-1}. This lattice periodicity, however, is not preserved, but the lamellar structure swells to a value of about 6.7 nm in the further time course of the relaxation process. In a last step, the coexisting rest-fraction of the original phase $L_{\beta'}$ and the swollen L_{α^*} phase (e.g. in Fig. 3A, 16th frame) transform in a continuous manner into the stable ripple phase $P_{\beta'}$ (Fig. 3A, 64th frame). The first-order reflection intensities of the L_{α^*} phase and the $L_{\beta'}$ phase and collapse into the (1, 1) reflection of the $P_{\beta'}$ phase at about 1/6.2 nm^{-1}. At the same time, the monoclinic lattice of the ripple phase becomes more and more expressed, which is seen in the increase of the (0, 1) reflection at 1/7.2 nm^{-1} (see Fig. 3B, frames 25–45).

Influence of salt concentration

In single-shot T-jump experiments the influence of NaCl (0, 0.5 and 1 M) on the lifetime and production of the L_{α^*} phase has been investigated (T_i = 27.5 °C). Table 2 gives the fit results to the proposed relaxation of the *d*-spacings (Eq. 1) within the first 3 s after the laser pulse, i.e., where the actual bilayer thickness is not larger that of the parent $L_{\beta'}$ phase, and the temperature change in the sample owing to thermal equilibration can be neglected (Kriechbaum et al. 1990). The relaxation kinetics are determined by a fast component, represented by the time constant τ_A, and a slow component, represented by τ_B. The fast component is only affected upon the addition of 1 M NaCl, but remains unchanged for the 0.5 M NaCl dispersion. More conclusive are the changes upon the time constant τ_B. Here, the relaxation process for both sodium chloride solutions (0.5 M and 1 M NaCl) is about three times longer compared to τ_B in pure water. The semi-logarithmic plot of the *d*-spacing relaxation, normalized with the *d*-value of the parent $L_{\beta'}$ phase d_0 (Fig. 4), verifies qualitatively these findings.

Table 2 also lists the maximum L_{α^*} phase fraction $\theta_{\alpha(max)}$, i.e., the amount of gel phase being transformed into the liquid-crystalline intermediate, for the cases of pure water, 0.5 M and 1 M NaCl. This parameter is found to decrease with increasing salt concentration, which is a further salt-induced effect.

Table 2 Temporal evolution of the *d*-spacing of the L_{α^*} phase during the pretransition of DPPC induced by a T-jump of 12 °C[a]

	d_0 (nm)	d_A (nm)	τ_A (s)	d_B (nm)	τ_B (s)	$d_{\alpha^* min}$ (nm)	$\theta_{\alpha(max)}$
No salt	6.37 ± 0.01	0.46 ± 0.03	0.053 ± 0.007	0.38 ± 0.02	1.06 ± 0.08	5.53 ± 0.06	0.95
0.5 M NaCl	6.40 ± 0.02	0.22 ± 0.03	0.06 ± 0.01	0.34 ± 0.01	3.2 ± 0.34	5.84 ± 0.06	0.85
1 M NaCl	6.45 ± 0.01	0.64 ± 0.06	0.13 ± 0.02	0.32 ± 0.03	3.8 ± 0.9	5.5 ± 0.1	0.75

[a] Fitting results (Eq. 1) for the T-jump experiments with an initial temperature of 27.5 °C on dispersions of 0, 0.5 and 1 M NaCl are given. Fits were performed for the first 3 s after the laser-shot, i.e., where the actual bilayer thickness meets the condition of not being larger than that of the parent $L_{\beta'}$ phase. The results were obtained by constraining d_0 to the mean value of the *d*-spacings of the first 10 frames before the laser shot, i.e., to the *d*-spacing of the gel phase. The value of minimum *d*-spacing of the intermediate $d_{\alpha^* min}$ is given by $d_{\alpha^* min} = d_0 - d_A - d_B$, which corresponds to the time $t = 0$. The maximum reached fraction of the liquid-crystalline intermediate is designated $\theta_{\alpha(max)}$. See also Fig. 4 for a graphical view of the results of the T-jump experiment

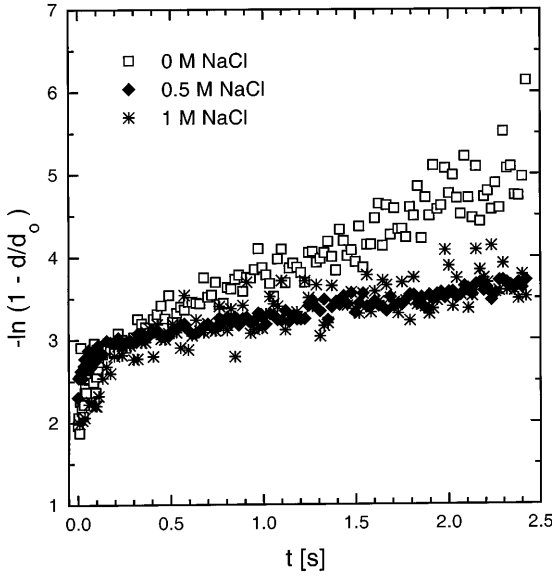

Fig. 4 Relaxation of the *d*-spacing of DPPC under the influence of 0, 0.5 and 1 M NaCl. The semi-logarithmic plot shows the temporal evolution of lattice parameter *d*, normalized with the *d*-value of the parent $L_{\beta'}$ phase, for the first 3 s after a T-jump of 12 °C. The samples were equilibrated at 27.5 °C beforehand. For fit results, see Table 2

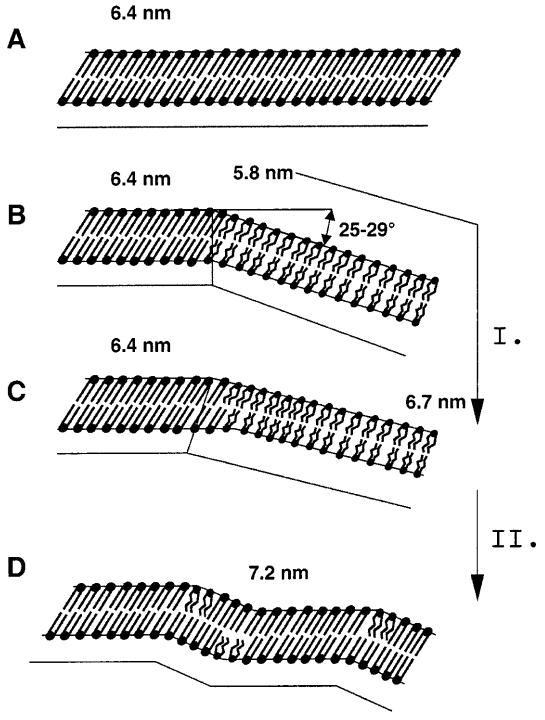

Fig. 5A–D Sketch of the main events during the pretransition in DPPC under non-equilibrium conditions. **A** The starting point for the T-jump is the gel-phase (chains shown with *straight lines*), in which the sample is allowed to equilibrate beforehand. **B** Directly after the laser flash, first, the generation of a thin liquid crystalline phase L_{α^*} (lipid-chain drawn with *kinked lines*) takes place coexisting with remaining amounts of the original gel phase $L_{\beta'}$. In the first milliseconds after the heating pulse the L_{α^*} phase has a *d*-spacing of 5.6–5.8 nm, that swells in a microsecond to second time scale until a *d*-spacing of about 6.7 nm is reached (**C**). In a second step (**C** to **D**), the aliphatic chains in the L_{α^*} phase relax to the all-*trans* conformation and the stable ripple phase $P_{\beta'}$ forms. For geometrical clearness the lipid as well as the water layers are depicted graphically, but only *d*-spacings of the first-order reflection are given explicitly

Discussion

In our previous investigations by fast time-resolved SAXS on the pretransition of phosphatidylcholines, we are able to demonstrate the occurrence of a short-lived, intermediate ordered state, with an anomalously thin but distinct lamellar repeat distance (Laggner et al. 1991). This earlier work, however, has left questions concerning the hydrocarbon chain packing. In order to clarify this point, we have undertaken the present simultaneous SAXS and WAXS studies, which were otherwise similar in terms of the T-jump relaxation approach as before. In correspondence to the SAXS pattern of the thin lamellar intermediate, we observe the occurrence of a broad diffuse WAXS peak at about $1/0.460\ nm^{-1}$ instantaneously with the T-jump (see Fig. 1). This indicates molten hydrocarbon chains, which is the attribute of phospholipids in the liquid crystalline phase. Hence, we conclude that the thin lamellar intermediate is a liquid crystalline phase (smectic A). Since the final temperature in the sample was always below the main transition temperature, the result is most surprising.

For a detailed description of the pretransition under non-equilibrium conditions we draw the following picture. Directly after the laser pulse – depending on the final temperature – various fractions the lamellar liquid crystalline phase L_{α^*} form (Fig. 5B). At the beginning of its existence (<5 ms), the lattice parameter with a value of 5.6–5.8 nm is clearly thinner as compared to the "normal" liquid crystalline phase L_α (6.7 nm at 44 °C; Rappolt 1995). This could be explained by a transient deficit of water directly after the laser pulse. The gel phase $L_{\beta'}$ has a water concentration of 25% w/w, whereas a completely saturated L_α phase contains at least 40% w/w (Kodama et al. 1982). Since time is too short for bulk water to penetrate through the bilayer stacks, the result of molten hydrocarbon chains, corresponding to the liquid crystalline phase, and the inter-bilayer water thickness, corresponding to the gel phase, will give a thin lamellar crystalline phase. This notion is supported by the following estimation based upon the above hypothesis: we approximate the water-layer thickness d_w of the intermediate by that of the original phase $L_{\beta'}$, which has a value of 1.3 nm at 20 °C (Nagle et al. 1996; Sun et al. 1994; Wiener et al. 1989). The bilayer thickness d_b of the liquid crystalline phase of DPPC, at 50 °C, has a value of about 4.5 nm (Janiak et al. 1979; McIntosh and Simon 1980; Nagle et al. 1996; Torbet and Wilkins 1976). Adding these two spacings results in a total lamellar repeat of 5.8 nm, which is within the measured range of 5.6–5.8 nm for the L_{α^*} phase directly after the laser pulse. This is of course

only a very rough estimate, since the water-layer thickness is probably underestimated by neglecting the increase of the lateral area per lipid molecule in the L_{α^*} phase, whereas the bilayer thickness is probably overestimated, because the number of *gauche* rotamers of the L_{α^*} phase below the main transition temperature is expected to be smaller compared to the fully hydrated L_α phase at 50 °C (Wilkinson and Nagle 1981).

Another striking argument for the manner of formation of the intermediate lamellar phase is given by a remarkable geometrical relationship. The arc-cosine relationship of 25–29° between the *d*-spacings of the L_{α^*} and the $L_{\beta'}$ phases right after the T-jump (Fig. 5B), is close to the tilt angle of the hydrocarbon chains in the $L_{\beta'}$ phase of about 30° (Kirchner and Cevc 1994; for a review see Tristram-Nagle et al. 1993). Therefore, we suggest that the first rapid step in the transition is a concerted disclination of the multilamellar system about a transition plane in the sense of a martensitic transformation (Laggner et al. 1991).

In the further time-course of the pretransition, the lattice of the L_{α^*} phase swells most probably by water uptake from the excess bulk water until a *d*-spacing is reached, which corresponds to the one of the "normal" L_α phase (Fig. 5C). This process can last up 3 s and is paralleled by a continuous increase of the fraction of the liquid-crystalline phase (Figs. 1 and 2). The time course compares well to diffusive and osmotic water permeation measurements on phosphatidylcholine vesicles in excess of water (Jansen and Blume 1995). Therefore, the water diffusion through the lamellae of the L_{α^*} phase is expected to be the rate limiting step in this process. This argument is underlined by the fact that the occurrence of the intermediate is one order of magnitude shorter with DMPC (1,2-dimyristoyl-*sn*-glycero-3-phosphocholine) as compared to DPPC (Laggner et al. 1991), which may be explained by altered diffusion barriers for water in both systems. While the thickness of the hydrophobic region should have only a minor influence on water permeability, the different occurrence of fluctuating lattice defects in DMPC and DPPC systems could be of considerable influence in the osmotically driven water flux (Jansen and Blume 1995).

As soon as the swelling of the liquid crystalline phase approaches its maximum, the coexisting phases $L_{\beta'}$ and L_{α^*} transform in a second step continuously into the stable ripple phase $P_{\beta'}$ (Fig. 5D). The last step is paralleled by an equilibration of the interbilayer water concentration, i.e., in the gel-phase domain the onset of faster chain and head group rotation will demand the uptake of water and in the liquid-crystalline domains the stiffening of the hydrocarbon chains will take place under the loss of water. The observations are summarized in the scheme of Fig. 6 and compared with the findings of the pretransition of phosphatidylcholines guided under near-equilibrium conditions.

Although the equilibrium state of the ripple phase has been studied in great detail since the 1970s, the conformation of the aliphatic chains still remains ambiguous.

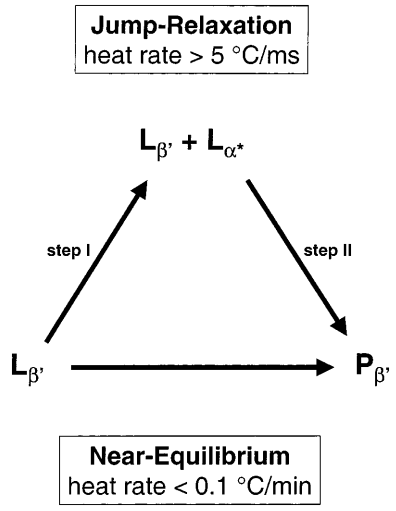

Fig. 6 Comparison of the observations for the two different approaches to the pretransition of DPPC. In contrast to the near-equilibrium technique, the structural pathway of the phase transitions under non-equilibrium conditions exhibits a lamellar crystalline intermediate L_{α^*}, although the main transition temperature is never passed over

Early X-ray diffraction experiments (Janiak et al. 1976; Tardieu et al. 1973) have provided evidence for all-*trans* conformation of the lipid chains, although some *gauche* conformers may be present (Ruocco and Shipley 1982). On the other hand, NMR studies indicate that in the $P_{\beta'}$ phase some chains adopt a conformation like the one in the liquid crystalline phase (Wittebort et al. 1981). Also, recent works on the structure of the ripple phase (Rappolt and Rapp 1996; Sun et al. 1996) strongly suggest a heterogeneous distribution of the lipid chain conformation: while the long side of the saw-tooth-like modulation of the $P_{\beta'}$ phase is similar to the gel phase layer, the bilayer along the short side appears to be slightly thinner (10–20%), with the electron density being lower in the headgroup region, as expected for a fluid bilayer with a larger molecular cross-section area. This idea, that the short side of the saw-tooth may partly consist of lipids with molten chains, fits very well with the events taking place under non-equilibrium conditions: the lamellar liquid crystalline intermediate L_{α^*} transforms after swelling to the thickness of the "normal" L_α phase together with various amounts of the lamellar gel phase $L_{\beta'}$ into the ripple phase $P_{\beta'}$. Hence, the ripple phase could incorporate both features, liquid crystalline and gel (Fig. 5D). This view is supported by a recently published model on the lipid pretransition (Heimburg 2000), where a coupling of the ripple phase formation with the main transition is considered. Here, the bending of the lipid bilayer is explained to be due to the formation of fluid one-dimensional line defects. Thus, the liquid crystalline intermediate can be seen as an attribute of the stable ripple phase, but just stronger pronounced.

Finally, the presence of salt should have an influence on the relaxation kinetics of the intermediate, as it is known that with high concentration of monovalent

cations the head groups tend to be oriented perpendicular to the lipid bilayer surface (Söderman et al. 1983), which changes the bilayer stability. The results show that, in the first 3 s after the T-jump, the relaxation process follows a two-component exponential decay. The first, fast process wherein the bilayer relaxes already to 50% of the starting value is nearly unaffected by the addition of salt (Table 2) and might be mainly driven by the strong steric repulsion of the head groups. The second, slower process, on the time scale of seconds, is prolonged by the addition of NaCl (Table 2 and Fig. 4). This may be explained, as argued above, by reduced permeability of the bulk solution owing to less defects. Further, the addition of sodium chloride reduces the T-jump-induced production of the L_{α^*} phase, because both the pre- and the main transition temperatures of phosphatidylcholine bilayers increase with salt concentration (Cevc 1991; Chapman et al. 1977; Träuble et al. 1976).

Acknowledgements This work has been supported by the ELETTRA-Project of the Austrian Academy of Sciences. M.R. is the recipient of a long-term grant from the European Commission under the program Training and Mobility of Researchers [contract no. SMT4-CT97-9024(DG12-CZJU)].

References

Albon N, Sturtevant JM (1978) Nature of the gel to liquid crystal transition of synthetic phosphatidylcholines. Proc Natl Acad Sci USA 75: 2258–2260

Amenitsch H, Rappolt M, Kriechbaum M, Mio H, Laggner P, Bernstorff S (1998) First performance assessment of the small-angle X-ray scattering beamline at Elettra. J Synchrotron Radiat 5: 506–508

Bernstorff S, Amenitsch H, Laggner P (1998) High-throughput asymmetric double-crystal monochromator for the SAXS beamline at ELETTRA. J Synchrotron Radiat 5: 1215–1221

Cevc G (1991) Polymorphism of bilayer membranes in the ordered phase and the molecular origin of lipid pretransition and rippled lamellae. Biochim Biophys Acta 1062: 59–69

Chapman D, Peel WE, Kingston B, Lilley TH (1977) Lipid phase transitions in model biomembranes. The effect of ions on phosphatidylcholine bilayers. Biochim Biophys Acta 464: 260–275

Gabriel A (1977) Position sensitive X-ray detectors. Rev Sci Instrum 48: 1303–1305

Heimburg T (2000) A model for the lipid pretransition – coupling of ripple formation with the chain melting transition. Biophys J 78: 1154–1165

Hendrix J, Koch MHJ, Bordas J (1979) A double focusing X-ray camera for use with synchrotron radiation. J Appl Crystallogr 12: 467–472

Janiak MJ, Small DM, Shipley CG (1976) Nature of thermal pretransition of synthetic phospholipids: dimyristoyl- and dipalmitoylphosphatidylcholine. Biochemistry 15: 4575–4580

Janiak MJ, Small DM, Shipley GG (1979) Temperature and compositional dependence of the structure of hydrated dimyristoylphosphatidylcholine. J Biol Chem 254: 6068–6078

Jansen M, Blume A (1995) A comparative study of diffusive and osmotic water permeation across bilayers composed of phospholipids with different head groups and fatty acyl chains. Biophys J 68: 997–1008

Jørgensen K (1995) Calorimetric detection of a sub-domain transition in long-chain phosphatidylcholine lipid bilayers. Biochim Biophys Acta 1240: 111–114

Kirchner S, Cevc G (1994) On the origin of the thermal $L_{\beta'} \rightarrow P_{\beta'}$ pretransition in the lamellar phospholipid membranes. Europhys Lett 28: 31–36

Klug HP, Alexander LE (1974) X-ray diffraction procedures: for polycrystalline and amorphous materials. Wiley, New York

Kodama M, Kuwabara M, Seki S (1992) Successive phase-transition phenomena and phase diagram of the phosphatidylcholine-water system as revealed by differential scanning calorimetry. Biochim Biophys Acta 689: 567–570

Komura S, Furukawa H (1988) Dynamics of ordering processes in condensed matter. Plenum Press, New York

Kriechbaum M, Laggner P, Rapp G (1990) Fast time-resolved X-ray diffraction for studying laser T-jump-induced phase transitions. Nucl Instrum Methods Phys Res A 291: 41–45

Laggner P (1993) Nonequilibrium phenomena in lipid membrane phase transitions. J Phys IV 3: 259–269

Laggner P, Kriechbaum M, Rapp G (1991) Structural intermediates in phospholipid phase transitions. J Appl Crystallogr 24: 836–842

Laggner P, Amenitsch H, Kriechbaum M, Pabst G, Rappolt M (1999) Trapping of short lived intermediates in phospholipid phase transitions: the L_{α^*} phase. Faraday Discuss Chem Soc 111: 31–40

Marsh D (1980) Molecular motion in phospholipid bilayers in the gel phase: long axis rotation. Biochemistry 19: 1632–1637

McIntosh TJ, Simon SA (1980) Hydration force and bilayer deformation: a reevaluation. Biochemistry 25: 4058–4066

Nagle JF, Zhang R, Tristram-Nagle S, Sun W-J, Petrache HI, Suter RM (1996) X-ray structure determination of the fully hydrated L_{α} phase dipalmitoyl-phosphatidylcholine. Biophys J 70: 1419–1431

Ohkura K, Kashino S, Haisa M (1972) Crystal structure of *p*-bromobenzoic acid. Bull Chem Soc Jpn 45: 2651–2653

Press WH, Teukolsky SA, Vetterling WT, Flannery BP (1986) Numerical recipes. Cambridge University Press, Cambridge

Pressl K, Jørgensen K, Laggner P (1997) Characterization of the sub-main-transition in distearoylphosphatidylcholine studied by simultaneous small- and wide-angle diffraction. Biochim Biophys Acta 1325: 1–7

Rapp G, Goody RS (1991) Light as a trigger for time-resolved structural experiments on muscle, lipids, p21 and bacteriorhodopsin. J Appl Crystallogr 24: 857–865

Rapp G, Rappolt M, Laggner P (1993) Time-resolved simultaneous small- and wide-angle X-ray diffraction on dipalmitoylphosphatidylcholine by laser temperature-jump. Prog Colloid Polym Sci 93: 25–29

Rapp G, Gabriel A, Dosire M, Koch MHJ (1995) A dual detector single readout system for simultaneous small- (SAXS) and wide-angle X-ray (WAXS) scattering. Nucl Instrum Methods Phys Res A 375: 178–182

Rappolt M (1995) Zeitaufgelöste Röntgenbeugung zur Untersuchung von Phasenübergängen an Modellmembranen. Thesis, University of Hamburg

Rappolt M, Rapp G (1996) Structure of the metastable ripple-phase of phosphatidylcholine. Eur Biophys J 24: 381–386

Ruocco MJ, Shipley GG (1982) Characterization of the sub-transition of hydrated dipalmitoylphosphatidylcholine bilayers. Kinetic, hydration and structural study. Biochim Biophys Acta 691: 309–320

Shepherd JWC, Büldt G (1979) The influence of cholesterol on head group mobility in phospholipid membranes. Biochim Biophys Acta 558: 41–47

Söderman O, Arvidson G, Lindblom G, Fontell K (1983) The interactions between monovalent ions and phosphatidylcholines in aqueous bilayers. Eur J Biochem 134: 309–314

Sun W-J, Suter RM, Knewtson MA, Worthington CR, Tristram-Nagle S, Zhang R, Nagle JF (1994) Order and disorder in the fully hydrated unorientated bilayers of gel phase dipalmitoylphosphatidylcholine. Phys Rev E 49: 4665–4676

Sun W-J, Tristram-Nagle S, Suter RM, Nagle JF (1996) Structure of the ripple phase in phosphatidylcholine. Proc Natl Acad Sci USA 93: 7008–7012

Tardieu A, Luzzati V, Reman FC (1973) Structure and polymorphism of the hydrocarbon chains of lipids: a study of phosphatidylcholine-water phases. J Mol Biol 75: 711–733

Tenchov BG, Yao H, Hatta I (1989) Time-resolved X-ray diffraction and calorimetric studies at low scan rates. I. Fully hydrated dipalmitoylphosphatidylcholine (DPPC) and DPPC/water/ethanol phases. Biophys J 56: 757–767

Torbet J, Wilkins MHF (1976) X-ray diffraction studies of phosphatidylcholine bilayers. J Theor Biol 62: 447–458

Träuble H, Teubner P, Woolley P, Eibl H (1976) Electrostatic interactions at charged lipid membranes. I. Effects of pH and univalent cations on membrane structure. Biophys Chem 4: 319–342

Tristram-Nagle S, Zhang R, Suter RM, Worthington CR, Sun W-J, Nagle JF (1993) Measurement of chain tilt angle in fully hydrated bilayers of the gel phase. Biophys J 64: 1097–1109

Wack DC, Webb WW (1989) Synchrotron X-ray study of the modulated lamellar phase $P_{\beta'}$ in the phosphatidylcholine-water system. Phys Rev A 40: 2712–2730

Wiener MC, Suter RM, Nagle JF (1989) Structure of the fully hydrated gel phase of dipalmitoylphosphatidylcholine. Biophys J 55: 315–325

Wilkinson DA, Nagle JF (1981) Dilatometry and calorimetry of saturated phosphatidylethanolamines dispersions. Biochemistry 20: 187–192

Wittebort RJ, Schmidt CF, Griffin RG (1981) Solid-state carbon-13 nuclear magnetic resonance of phosphatidylcholine gel to liquid-crystalline phase transition. Biochemistry 20: 4223–4228